

Fractal properties of SYM-H during quiet and active times

James Wanliss

Department of Physical Sciences, Embry-Riddle Aeronautical University, Daytona Beach, Florida, USA

Received 15 April 2004; revised 6 December 2004; accepted 14 December 2004; published 4 March 2005.

[1] Detrended fluctuation analysis was applied to the magnetic storm index SYM-H for the epoch 1981–2002. The objective was to determine the characteristic fractal statistical differences, if any, between a quiet and active magnetosphere. The entire data set comprises over 11 million points that include numerous intervals that can be classified as quiet or active. For quiet intervals we required $Kp \leq 1$ for 10,000 consecutive minutes. Similarly, to qualify as an active interval required $Kp \geq 4$ for 10,000 consecutive minutes. All active intervals included magnetic storms. Detrended fluctuation analysis was applied to each of these intervals to obtain local scaling exponents. A clear difference in statistical behavior during quiet and active intervals is implied through analysis of the scaling exponents for the quiet and active intervals; active intervals generally have larger values of scaling exponents. This implies that although SYM-H appears monofractal on shorter timescales, it is more properly described as a multifractal Brownian motion. An overall trend toward higher scaling exponents was also discovered for increasing magnetospheric activity, possibly implying an increase in organization with magnetospheric activity. The overall distribution of the scaling exponents for active intervals was Gaussian. For quiet intervals, however, it was bi-Gaussian, perhaps indicative of different internal (magnetospheric) and external (solar wind) nonlinear forcings.

Citation: Wanliss, J. (2005), Fractal properties of SYM-H during quiet and active times, *J. Geophys. Res.*, *110*, A03202, doi:10.1029/2004JA010544.

1. Introduction

[2] Magnetic storms, characterized by global geomagnetic disturbances, result from the interaction between magnetized plasma that propagates away from the Sun and the near-Earth space plasma environment. *Chapman* [1919] placed the global aspect of storms on a firm footing when he used ground-based magnetometers to demonstrate that for some time after great geomagnetic disturbances and auroral activity the horizontal component of the magnetic field around the world is significantly reduced from its average. Storms frequently begin with a sudden worldwide increase in the magnetic field by tens of nanotesla that lasts several minutes to several hours, known as the initial phase. Following the initial phase comes the main phase, which typically lasts about a day, and features large reductions in the horizontal component on the order of hundreds of nanotesla. Subsequent to the main phase the worldwide horizontal magnetic field slowly returns to prestorm values during a recovery phase that lasts several days. With the onset of the space age it became apparent that “magnetic storm” was perhaps too colloquial a term for what was discovered to be a massive-scale geospace phenomenon, which could be called a space storm.

[3] Magnetic storms characterize the most dynamic magnetospheric behavior. They include a rich diversity of complex electromagnetic processes extending from the surface of the Earth into the magnetosphere, with the primary locus of activity being in the near-Earth geospace environment [*Baker et al.*, 1997; *Li et al.*, 1997; *Reeves*, 1998]. These include energetic particle injection and precipitation [*Reeves and Henderson*, 2001; *Horne and Thorne*, 2003], acceleration of relativistic electrons [*Li et al.*, 2001; *Summers et al.*, 2002; *Meredith et al.*, 2003], ring current enhancement, decay, and composition changes [*Daglis et al.*, 1999; *Liemohn et al.*, 2001; *Kozyra et al.*, 2002]. Recent studies on the causes of magnetic storms have found that coronal mass ejections and extreme values of the southward interplanetary magnetic fields appear to be key factors in storm development [*Tsurutani et al.*, 1992; *Gonzalez et al.*, 1994; *Kamide et al.*, 1998; *Richardson et al.*, 2001]. Coupling and feedback between the ionosphere and magnetosphere also plays an important role in the initiation and development of magnetic storms, and interaction between these two spheres is highly nonlinear [*Lui*, 2002; *Daglis et al.*, 2003, and references therein]. Storms thus form a complex system of nonlinear phenomena that include components of solar and terrestrial origin [*Benkevitch et al.*, 2002; *Daglis et al.*, 2003].

[4] The most widely used statistical descriptor of magnetic storm activity is the *Dst* index. This index is considered to reflect variations in the intensity of the symmetric part of the ring current that circles Earth at altitudes ranging

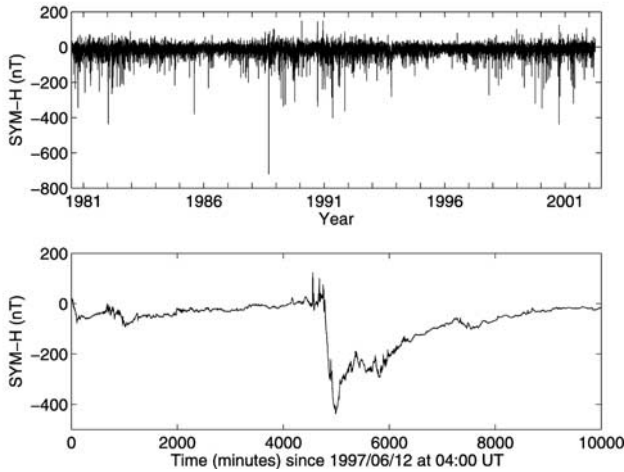


Figure 1. (top) SYM-H time series from 1981 to 2002 fluctuating around a zero mean with large intermittent negative perturbations. (bottom) 10,000 min of SYM-H data from a magnetic storm during 1997 appearing to feature long-range dependence.

from about 3 to 8 Earth radii (R_E) and is related to the total energy in the drifting particles that form the ring current. It is calculated as an hourly index from the horizontal magnetic field component at four observatories, namely, Hermanus (33.3°S, 80.3° in magnetic dipole latitude and longitude), Kakioka (26.0°N, 206.0°), Honolulu (21.0°N, 266.4°), and San Juan (29.9°N, 3.2°). These four observatories were chosen because they are close to the magnetic equator and thus are not strongly influenced by auroral current systems. Convolution of their magnetic variations forms the *Dst* index, measured in nanotesla, which is considered to provide a reasonable global estimate of the variation of the horizontal field near the equator. It is calculated once every hour.

[5] Another ground-based magnetic index called SYM-H was developed as part of an effort to describe geomagnetic disturbance fields at midlatitudes with high-time resolution. It is essentially the same as the *Dst* index, although it uses 1-min values from a different set of stations and a slightly different coordinate system. As such, this index also provides an excellent measure of the large-scale behavior of the ring current and magnetic storm dynamics (World Data Center for Geomagnetism, Kyoto, Mid-latitude geomagnetic indices “ASY” and “SYM” for 1999 (provisional), available at <http://swdcwww.kugi.kyoto-u.ac.jp/aeasy/asy.pdf>).

[6] The statistics of the magnetic storm fluctuations observed on the ground are related to magnetospheric-ionospheric coupling and feedback, relaxation and energization processes, and transport phenomena in space plasmas. It is apparent from Figure 1 that the SYM-H time series displays evidence of both long-range dependence and intermittency. The large, intermittent negative spikes in SYM-H correspond to intervals of intense magnetic storms. In this paper the statistical nature of the nonlinear scaling properties in SYM-H are examined in detail over two solar cycles to determine the characteristic statistical differences, if any, between magnetospheric dynamics during intervals

defined as quiet and active. The idea being pursued here, in greater detail than before, is that statistically stable, but dissimilar, nonlinear processes are involved in quiet and active periods [Wanliss, 2004]. If this is the case, the transition from quiet to active intervals should be indicated by a change in the statistical variability which could be used to predict the onset of active periods.

[7] In the present work, the goal was to determine whether the nonlinear statistics of SYM-H data during quiet intervals are similar, and whether the nonlinear statistics of active intervals also cluster around common values. Based on the analysis of 22 years of 1-min SYM-H data (over 11 million data points), we demonstrate that, on average, intervals that are described as quiet and active are each well described by a single nonlinear scaling exponent, characteristic of fractional Brownian motion (fBm). However, on average, quiet and active intervals follow significantly different power law scaling behaviors.

[8] The fractal analysis technique followed in this paper, namely, detrended fluctuation analysis (DFA), is discussed in section 2. Section 3 considers the subset of the SYM-H time series that is selected for analysis and how we decided which events were quiet and which were active. Results from the data analysis are discussed in section 4. Section 5 gives our conclusions, suggesting that the SYM-H time series may be better described as a multifractional Brownian motion (mFBm), and discusses the implications of this result.

2. Method of Analysis

[9] A signal that displays fBm is one that has a zero mean and which can be expressed as the stochastic integral [Mandelbrot and Van Ness, 1968]

$$B_\alpha(t) = \frac{1}{\Gamma(\alpha + 1/2)} \left\{ \int_{-\infty}^0 [(t-s)^{\alpha-1/2} - (-s)^{\alpha-1/2}] dW(s) + \int_0^t (t-s)^{\alpha-1/2} dW(s) \right\}, \quad (1)$$

where Γ is the gamma function and W is a white noise process defined on $(-\infty, \infty)$. Here $\alpha \in (0, 1)$ is the scaling exponent. Larger values closer to 1 result from signals that are relatively smooth, and smaller values closer to 0 are very rough. The covariance function for the fBm signal is given by

$$\text{cov}\{B_\alpha(s), B_\alpha(t)\} = \frac{1}{2} \left\{ |s|^{2\alpha} + |t|^{2\alpha} - |s-t|^{2\alpha} \right\}, \quad (2)$$

so that $B_\alpha(0) \equiv 0$ and the variance $\text{var}\{B_\alpha(t)\} = t^{2\alpha}$. This means that for the special case $\alpha = 1/2$, fBm reduces to the well-known random walk. Signals with scaling exponents above $\alpha = 1/2$ are also called persistent, because if the data at some point have $B(t_{i+1}) > B(t_i)$, for example, then the probability is >0.5 that $B(t_{i+2}) > B(t_{i+1})$. Signals with exponents below $1/2$ are called antipersistent because if $B(t_{i+1}) > B(t_i)$, the probability is >0.5 that $B(t_{i+2}) < B(t_{i+1})$. Typically, fBm is nonstationary, and thus detection of the

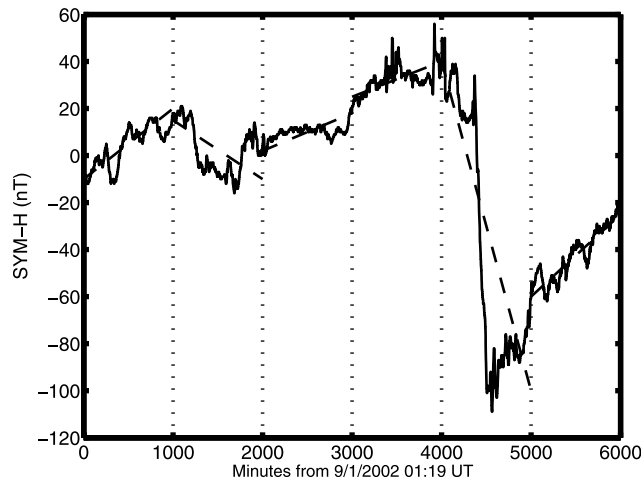


Figure 2. 6000 min of SYM-H data. Vertical dotted lines indicate boxes of size $n = 1000$, and the dashed curve segments represent the trend estimated in each box by a least squares fit. In this example the trend function is linear.

presence of memory is a delicate task. Nonstationarity means that the statistical properties are not constant through the signal, and traditional analysis methods, that assume stationarity (e.g., power spectra), cannot be used. Notwithstanding the difficulties, fBm has been observed in a variety of fields, including hydrology [Neuman and Di Federico, 2003], geophysics [Frisch, 1997], biology [Collins and De Luca, 1994], telecommunication networks [Taqqu et al., 1997], and others.

[10] Figure 1 (top) shows the entire 22-year SYM-H time series used in this study. Figure 1 (bottom) shows a small subset of 10,000 min from the SYM-H series. Figure 1 (top) gives evidence of intermittency, and Figure 1 (bottom) of long-range dependence. Long-range correlations in the SYM-H time series can be tested for in numerous ways. A general methodology is to estimate how a fluctuation measure, denoted here by F , scales with the size n of the time window considered. Specific methods, such as Hurst's rescaled range analysis [Hurst, 1951], power spectral analysis, structure function analysis [Abramenko et al., 2002], or detrended fluctuation analysis [Peng et al., 1995], all essentially calculate such a fluctuation measure, although the measure is different for each technique. Typically, $F \propto n^\alpha$, where α is the scaling exponent. For a time series that follows a fBm the relationships between the scaling exponents of the various methods are simple.

[11] Burlaga and Klein [1986] showed that in some cases the components and magnitude of the interplanetary magnetic field have properties of fBm and that frequently there are deeper symmetries in the large-scale magnetic field strength fluctuations [Burlaga, 1991]. The scaling properties of space physics data during dynamic magnetospheric activity were investigated by Ohtani et al. [1995]. They found that magnetic fluctuations in the magnetotail were well described as self-affine data whose spectrum follows a power law. Studies of geomagnetic indices and ground-based data have served as particularly fruitful examples of fBm in space physics [Sharma, 1995; Consolini and Lui,

2000; Price and Newman, 2001; Wanliss and Reynolds, 2003].

[12] We will employ a DFA to the SYM-H data. Novel ideas from statistical physics led to the development of DFA [Peng et al., 1995]. The method is a modified root mean squared analysis of a random walk designed specifically to be able to deal with nonstationarities in nonlinear data and is among the most robust of statistical techniques designed to detect long-range correlations in time series [Taqqu et al., 1996; Cannon et al., 1997; Blok, 2000]. DFA has been shown to be robust to the presence of trends [Hu et al., 2001] and nonstationary time series [Kantelhardt et al., 2002; Chen et al., 2002].

[13] Briefly, the methodology begins by removing the mean, \bar{B} , from the time series, $B(t)$, and then integrating

$$y(k) = \sum_{t=1}^k [B(t) - \bar{B}]. \quad (3)$$

[14] The new time series is then divided into boxes of equal length, n (Figure 2). The trend, represented by a least squares fit to the data, is removed from each box; the trend is typically a linear, quadratic, or cubic function [Hu et al., 2001; Vjushin et al., 2001]. In this paper we use a quadratic function which eliminates errors due to linear trends in the data. Box n has its abscissa denoted by $y_n(k)$. Next the trend is removed from the integrated time series, $y(k)$, by subtracting the local trend, $y_n(k)$, in each box.

[15] For a given box size n , the characteristic size of the fluctuations, denoted by $F(n)$, is then calculated as the root mean squared deviation between $y(k)$ and its trend in each box:

$$F(n) = \sqrt{\frac{1}{N} \sum_{k=1}^N [y(k) - y_n(k)]^2}. \quad (4)$$

[16] This calculation is performed over all timescales (box sizes). A power law scaling between $F(n)$ and n indicates the presence of scaling:

$$F(n) \propto n^\alpha, \quad (5)$$

where the parameter α is a scaling exponent. Given a fractional Brownian motion series, the scaling exponent $\alpha = H$, the familiar Hurst exponent [Mandelbrot and Van Ness, 1968]. If $\alpha = 0.5$, the signal is white noise; $\alpha < 0.5$ indicates antipersistence, and $\alpha > 0.5$ indicates a persistent time series.

3. Observations

[17] The goal of our study was to determine whether the nonlinear statistics of SYM-H data during quiet intervals are significantly different than those from active intervals. In addition, if it was found that nonlinear statistics for quiet intervals and active intervals generally cluster around certain values, we wished to determine whether the statistics are significantly different for quiet and active intervals. To ensure that data selected were representative of a magnetospheric quiet or active state, we used SYM-H as well as the

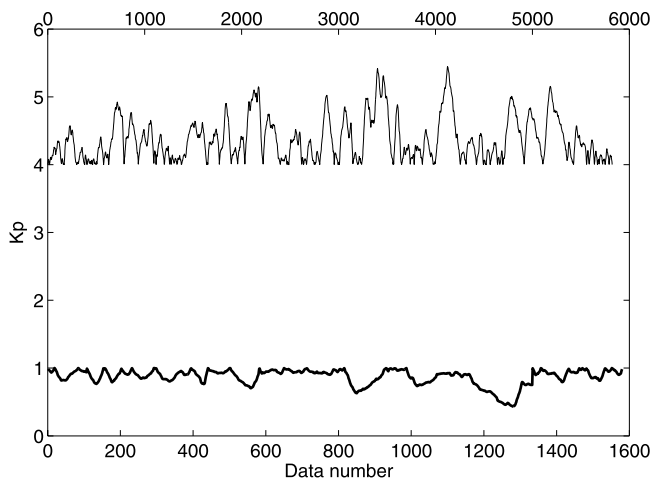


Figure 3. Smallest (bottom plot of 1580 data points) and largest (top plot of 5823 data points) mean values of Kp for each data subset, comprising 10,000 consecutive minutes, selected for 1981–2002.

Kp index selection criteria. When SYM-H indicates significant activity, there is usually significant Kp activity also. Since SYM-H is calculated exclusively from low- to middle-latitude magnetometer stations, and Kp includes higher-latitude stations, quiet interval data selection based on Kp ensures that data are selected when the entire magnetosphere is likely to be as close as possible to a ground state.

[18] On the other hand, during active times such as magnetic storms, Kp is generally large, and SYM-H reaches large negative values. However, sometimes SYM-H shows only small activity even when Kp is large, demonstrating dynamic activity (for example, magnetospheric substorms) at higher-latitude regions of the magnetosphere. This does not imply that some events classified as active are really substorms, since substorms typically result in $Dst > -30$ nT [Gonzalez *et al.*, 1994], but the smallest value found in our data set is -60 nT. In addition, the timescale employed here, namely 10,000 min, ensures that more than substorms

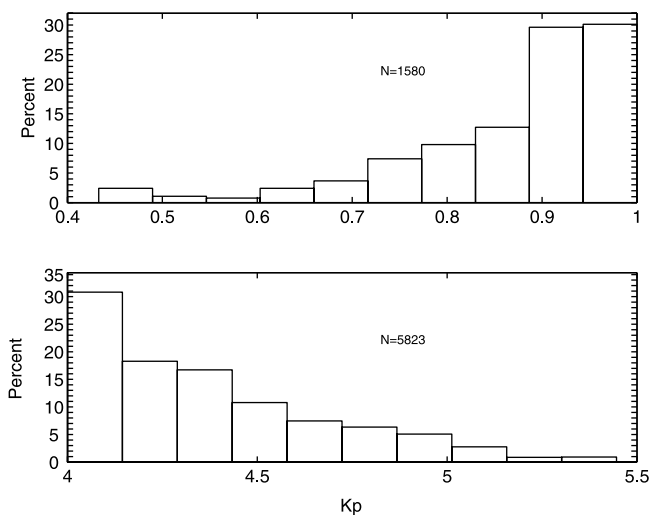


Figure 4. Histograms of the mean Kp value for the selected (top) quiet and (bottom) active events.

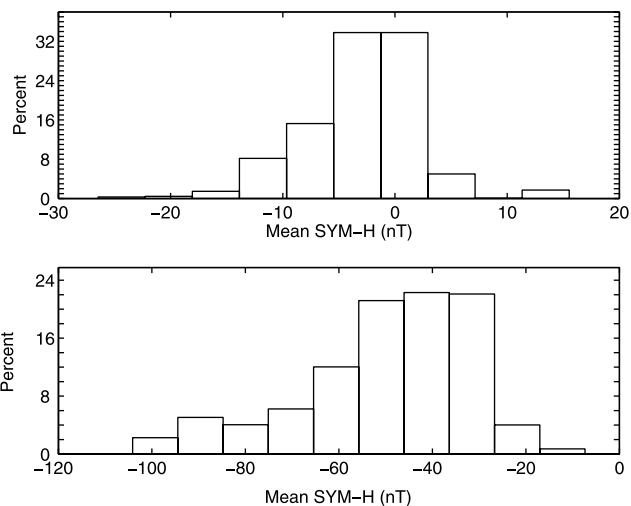


Figure 5. Mean SYM-H values for (top) all quiet data intervals and (bottom) all active intervals.

are being observed, as the timescale of substorms are a few hours. All of this means that for our data set, active events are at least moderate storms, or more active. It also implies, as is well known, that substorms are a frequent occurrence during storms. Use of Kp to select events ensures that data are selected when the magnetosphere is truly quiet or active over a wide range of latitudes.

[19] To ensure that the computation of the scaling exponent was robust, data subsets were selected that had 10,000 data points. For quiet intervals, we required $Kp \leq 1$ for 10,000 consecutive minutes. Similarly, to qualify as an active interval required $Kp \geq 4$ for 10,000 consecutive minutes. This definition of quiet and active intervals is well supported by previous studies [e.g., Rangarajan and Iyemori, 1997] and follows the classification system suggested by Bartels [1963]. Out of the original SYM-H time series of over 11 million data points, we were able to identify 5823 active intervals and 1580 quiet intervals that satisfied our criteria when overlapping intervals were allowed. When entirely independent events only were allowed, we found 76 active and 30 quiet intervals. In the text immediately following, we discuss analysis for the events with overlapping data. In Figure 3 we show the mean values of Kp for all of the selected intervals with overlapping data. The top axis and topmost time series refers to the active intervals, and the bottom axis and time series refers to the quiet intervals. As shown by Rangarajan and Iyemori [1997], the quiet intervals typically show peak occurrences during solar minimum years. As well, we found that the period 1981–2002 is clearly rather active, with it being more rare to find quiet intervals than active intervals [Rangarajan and Iyemori, 1997]. Even so, since there are over 1500 quiet intervals, this will be adequate for robust statistical comparison. Figure 4 shows the corresponding histograms of the mean Kp values. The majority of events cluster around the limits $Kp = 4$ (active) and $Kp = 1$ (quiet).

[20] It is clear from Figure 5, which shows the corresponding average SYM-H values for each selected event, that most “quiet” events, as determined via Kp , correspond to very small average SYM-H values as well, with no average more negative than -30 nT. The “active”

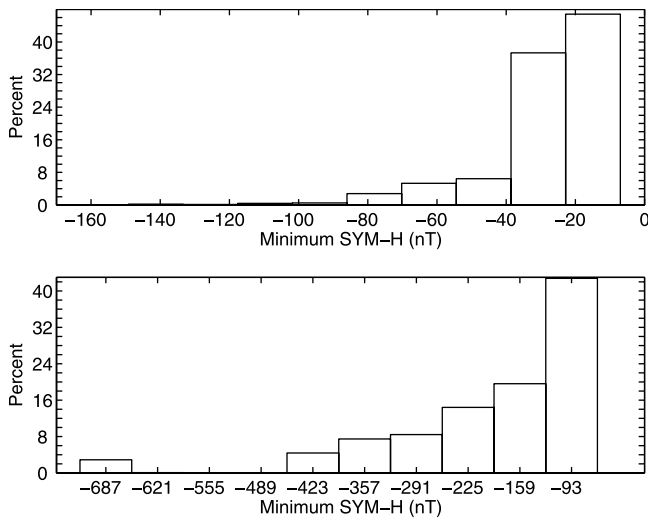


Figure 6. Minimum SYM-H values for (top) quiet and (bottom) active intervals.

events correspond to rather larger average values, although there are a number of events that have averages that could be considered on the small side. Comparison in terms of magnetic storm categorization is useful at this point. Storms are very sensitive to strong dawn-to-dusk electric fields, which are the product of the southward directed interplanetary magnetic field and the solar wind velocity. *Gosling et al.* [1991] demonstrated that storms in the intense category are typically caused by southward magnetic fields within higher-speed streams led by shocks, although these factors are not sufficient or necessary for storm development [Gonzalez et al., 1994; Kamide et al., 1998]. Table 1 shows threshold values that are required to produce storms at an 80% occurrence level; for example, intense storms will occur 80% of the time if $B_S > 10$ nT for 3 hours or more. Figure 6, which shows the minimum value of SYM-H for each selected interval, can be understood in terms of this categorization. These bar graphs show that all active intervals exceed magnetic storm thresholds given in Table 1 and that most (4577 events = 79%) qualify as intense storms; the rest (1246 events = 21%) of the active events qualify as moderate storms, with the least negative value of SYM-H = -60 nT. No small storms are included in the active event database.

[21] Intervals classified as quiet, in terms of Kp , are a little more complicated, as 15 events (1%) have minimum SYM-H values below -100 nT (Figure 6) and thus actually qualify as intense storms! A further 157 “quiet” events (10%) qualify as moderate storms, and 223 events (14%) are small magnetic storms. This leaves a total of 1185 events (75%) that are not magnetic storms, per the classification in Table 1, and which could be considered truly representative of a quiet magnetospheric state.

[22] As mentioned previously, in many cases the Kp criterion was satisfied for more than 10,000 consecutive minutes. When this happened, each interval of length 10,000 min that was used to compute a scaling exponent was allowed to include overlapping data from other adjacent intervals. When no overlapping data are allowed (completely independent intervals), there are only 76 inde-

Table 1. Threshold for Storms at 80% Occurrence Level^a

Storm Type	Dst , nT	B_S , ^b nT	dT , ^c hours
Intense	-100	10	3
Moderate	-50	5	2
Small	-30	3	1

^aAfter Gonzalez et al. [1994].

^bSouthward interplanetary magnetic field.

^cLength of time when the interplanetary magnetic field has values above the required threshold.

pendent active intervals and 30 independent quiet intervals. In what follows, two individual events are considered, followed by analysis on events with overlapping data and finally by analysis of independent events.

4. Data Analysis

4.1. Individual Events

[23] In this section we demonstrate detailed analysis of a quiet and an active interval. We will then calculate averages of scaling exponents for all active and all quiet intervals. In Figure 7 we show the SYM-H values for the quiet interval on 12 June 1997. This event features very low, small values of SYM-H (mean = 0.19 nT, minimum = -10 nT); the average $Kp = 0.94$. The scale is very wide for comparison to the active interval. The log-log plot of fluctuation versus box size, calculated from DFA, is given in Figure 8. The solid curve is the best-fit linear curve to the data (shifted). The dotted curve, shown for reference, has a slope $\alpha = 0.50$, corresponding to a random walk. The actual fluctuations for the quiet interval (circles) follow clear power law scaling over ~ 2 decades ($16 \leq n \leq 1000$), with scaling exponent $\alpha = 0.52 \pm 0.04$, whereafter the data appear more variable. This variability highlights one difficulty in this analysis, namely that the low and high box-number edges should be treated with caution. The first few points at the low end should be disregarded because in this region the detrending removes too much of the fluctuation. For larger values of box size, there are too few boxes for a proper averaging to be made, and we also disregard those values.

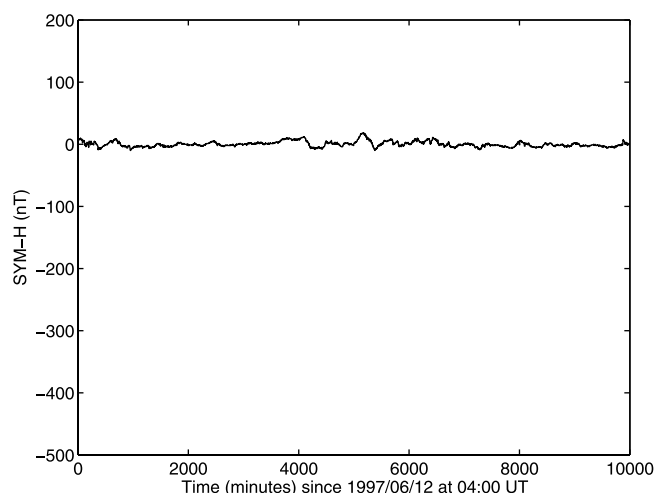


Figure 7. An example of SYM-H during a quiet period selected on 12 June 1997. Scale is selected for ease of comparison with the active period data shown in Figure 9.

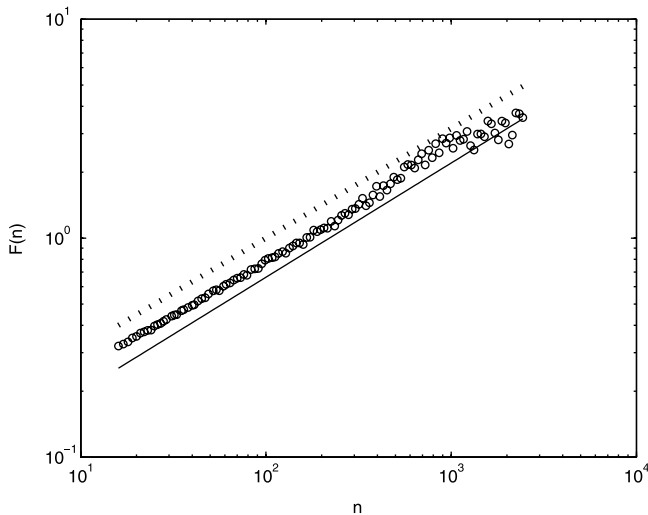


Figure 8. Circles showing the fluctuation versus box size for the quiet event beginning at 0400 UT on 12 June 1997. Dotted curve has a slope of 0.5 and is shown for reference purposes. Solid curve is the best fit linear curve to the data (shifted) and has a slope $\alpha = 0.52 \pm 0.04$.

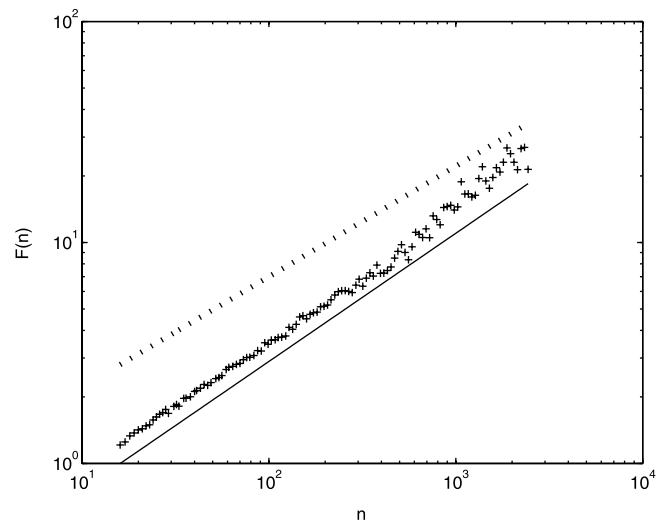


Figure 10. Pluses showing the fluctuation versus box size for the active event beginning at 2100 UT on 27 March 2001. Dotted curve has a slope of 0.5 and is shown for reference purposes. Solid curve is the (shifted) best fit linear curve to the data, with a slope $\alpha = 0.58 \pm 0.1$.

In practice, all best linear fits have thus been made for $16 \leq n \leq 1024$.

[24] Data for the active interval beginning at 2100 UT on 27 March 2001 are shown in Figure 9. This is a classic sudden onset magnetic storm signature in SYM-H (mean = -72.3 nT, minimum = -437 nT); the average $Kp = 4.02$ for this event. Figure 10 shows the log-log plot of fluctuation versus box size. The dotted curve shows the reference curve, which has $\alpha = 0.50$, as before. As in the quiet case, the fluctuations for the active interval (pluses) follow a power law scaling over two decades, with $\alpha = 0.58 \pm 0.1$.

[25] The fact that the scaling exponent is different for the active and quiet interval gives some indication that their nonlinear statistical behavior is dissimilar. Whereas the quiet event is consistent with Brownian motion, the active event result is quite different and is more consistent with

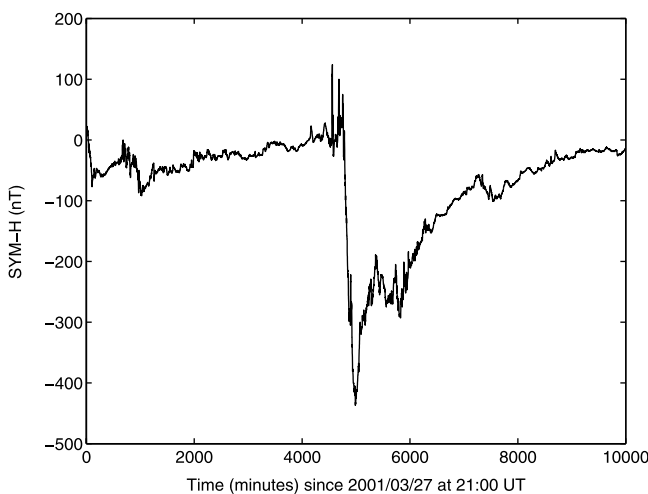


Figure 9. An example of SYM-H during an active period selected on 27 March 2001.

correlated behavior. We now turn to the analysis of multiple events, a prerequisite for arriving at any reliable conclusions about the significance of this apparent difference between active and quiet intervals.

4.2. Statistics for Overlapping Intervals

[26] All in all, the number of continuous intervals that satisfy the Kp criteria for longer than 10,000 min are 30 and 76, for quiet and active intervals, respectively. When the selection criterion was satisfied for more than 10,000 min, every additional minute where the Kp criterion was satisfied allowed computation of a new scaling exponent. When overlapping intervals are allowed, i.e., when quiet and active intervals include data from other intervals, the total number of active and quiet intervals is 5823 and 1580, respectively. Addition of extra intervals allows for smaller uncertainties once averages are calculated but raises the question of bias in the statistical results due to oversampling.

[27] Oversampling is certainly an issue for traditional methods which study the moments of the distribution of measured values, e.g., averages, standard deviations, and distribution functions. When looking at overlapping data, it can be demonstrated that the variation of these parameters will be smooth and will result in bias in subsequent averages. However, in the case of this present analysis where the scaling exponent is calculated through nontrivial convolution of data and graphical fitting, the degree of bias is not so obvious, although some bias must be present. Previous work by Wanliss [2004] suggests that the scaling exponents for SYM-H are a function of time; $\alpha = \alpha(t)$. This is not entirely surprising since the signals are obtained under constantly varying conditions. This implies that it is not clear a priori that allowing overlapping intervals will result in a large skewing of the average results, as is the case when averages are found from moments. The moments, and distribution, of the original data are preserved in the DFA

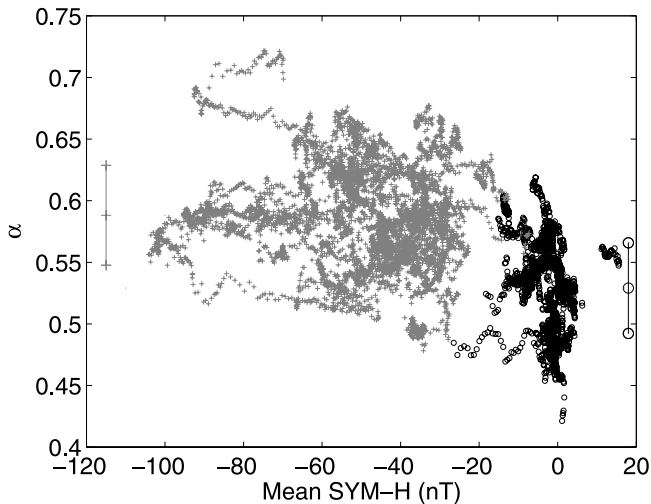


Figure 11. Comparison of computed α for quiet (dark circles) and active (light pluses), as a function of mean SYM-H value for the data interval. Intervals allow overlapping data. Quiet and active interval results cluster around different mean values, $\alpha_Q = 0.53 \pm 0.04$ and $\alpha_A = 0.59 \pm 0.04$, respectively. Average values are indicated by the vertical lines to the left and right sides of the plot.

method. Unlike the moments, the scaling exponent is strongly dependent on the order in which the data are found. For example, in experiments on synthetic fBm we found in cases that even a 1% (100 data points) difference in data can result in a 0.1 change in the measured scaling exponent. Since “local” changes in scaling exponents can be observed through DFA, it may be important to consider all intervals

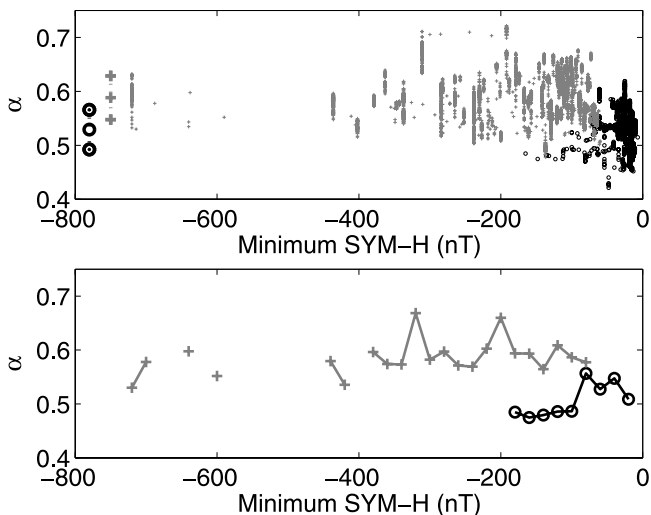


Figure 12. (top) Comparison of computed α for quiet (dark circles) and active (light pluses), as a function of minimum SYM-H value for the data interval. Mean α values are shown by the vertical lines to the left of the plot. Quiet and active intervals cluster around different mean values, $\alpha_Q = 0.53 \pm 0.04$ and $\alpha_A = 0.59 \pm 0.04$, respectively. (bottom) Averaged values of α in boxes of 20-nT width demonstrating the clear separation between the statistics for quiet (dark circles) and active (light pluses) intervals.

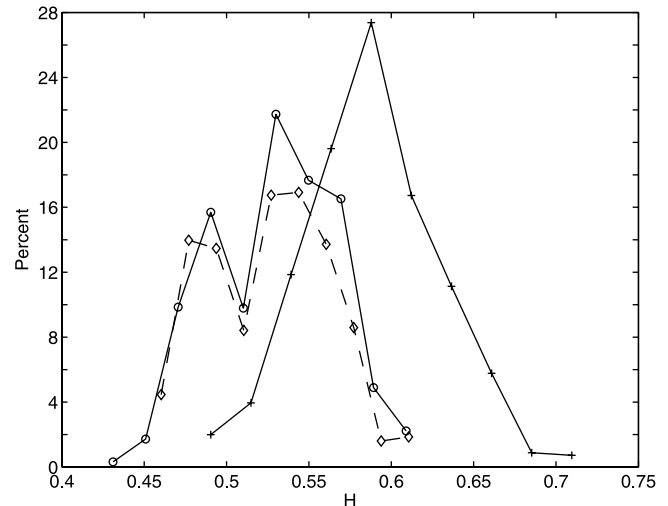


Figure 13. Probability distributions of the scaling exponents for active (pluses) and quiet (circles) events on a log scale. Results are from data that allowed overlapping intervals. Results from quiet events that had SYM-H > -30 nT are shown as diamonds.

to get a full view of the nonlinear characterization of SYM-H. In fact, several studies have insisted on overlapping intervals in order to obtain local measurements of the degree of long-range correlations [e.g., Vandewalle and Ausloos, 1997; Muniandy *et al.*, 2001]. Notwithstanding these considerations, it will be necessary to apply the analysis to completely independent intervals, as only this can dispel the questions of bias raised through the use of overlapping intervals. If significant bias results from overlapping intervals, then the distribution of scaling exponents should be quite different from the case with only independent intervals. Otherwise, the distribution should be similar, although better resolved for overlapping intervals, because there are more data.

[28] For overlapping intervals, good discrimination between the quiet and active groups of data was achievable through the observation of the scaling exponents for all events. Figure 11 shows a comparison of computed exponents for quiet (dark circles) and active (light pluses) events, as a function of mean SYM-H value for the data interval. The quiet and active intervals cluster around different mean values, $\alpha_Q = 0.53 \pm 0.04$ and $\alpha_A = 0.59 \pm 0.04$, respectively. Figure 12 shows a similar comparison, but in terms of the minimum SYM-H during the data interval. Figure 12 (top) shows all data results for quiet (dark circles) and active (light pluses) values of α . Clustering of quiet and active events indicates that active events tend to have larger scaling exponents. The mean values and standard deviation error bars are shown bolded at the left of the plot. To more clearly make the distinction between quiet and active intervals, Figure 12 (bottom) has averaged the α values over boxes of 20-nT width. These plots demonstrate that there is a clear separation between the statistics for quiet and active intervals. In answering the question of significance of the difference of the means, we consider the entire distribution of quiet and active interval scaling exponents. We have, in this analysis, two separate distributions of scaling

Table 2. Scaling Exponents Calculated by Fitting Statistics From Active Times to a Gaussian Distribution Function and Quiet Times to a Bi-Gaussian Distribution Function^a

Data Type		N	α	α_1	α_2
Quiet intervals	intense storms	15	0.49 ± 0.02	0.48 ± 0.01	$0.52 \pm 0.00(1)$
	moderate storms	157	0.54 ± 0.04	0.52 ± 0.03	0.59 ± 0.01
	small storms	223	0.54 ± 0.03	0.47 ± 0.04	0.54 ± 0.02
	truly quiet	1185	0.53 ± 0.04	0.49 ± 0.02	0.55 ± 0.02
	all	1580	0.53 ± 0.04	0.48 ± 0.01	0.54 ± 0.03
Active intervals	intense storms	4558	0.59 ± 0.04		
	moderate storms	1324	0.58 ± 0.04		
	all	5882	0.59 ± 0.04		

^a N , number of events; α , mean scaling exponent; α_1 and α_2 , computed exponents for the bi-Gaussian quiet distribution function.

exponents (Figure 13). These distributions have different means and overlap in their tails.

[29] It is important to note that the overlap in the standard deviation error bars does not imply that results are statistically insignificant. The standard deviation quantifies variability but does not account for sample size. To assess statistical significance, one must take into account sample size and variability. Observing whether standard deviation error bars overlap or not tells one nothing about whether the difference in means is, or is not, statistically significant, and other significance tests must be used. A Student's t test compares one variable between two groups. It is a test for measuring the significance of a difference of means between two distributions and is ideally suited to determine whether the two distributions (scaling exponents from quiet and active intervals) are from the same population. The null hypothesis is that the scaling exponents from quiet and active intervals are from the same distribution, and any differences are due purely to randomness. The important output of the t test is the value of p , which is the probability that the difference in the means of the two distributions being compared is due to random variation. To determine whether these averaged scaling exponents for quiet and active intervals were significantly different from the null hypothesis, we applied a Student's t test and found $p < 10^{-5}$. These results imply that the difference between the average scaling exponent computed for quiet and active intervals is statistically significant.

[30] In Figure 13 we show the normalized probability distribution function for the statistics computed for the 5823 active intervals and 1580 quiet intervals. Data have been normalized for this plot so that the probabilities are expressed as percentages. The distribution of the active interval scaling exponents (pluses) is Gaussian, but the quiet intervals (circles) have two populations that are best fit as a bi-Gaussian. Since we found that the selection criteria did result in some events being classified as quiet, even though SYM-H values indicated the presence of a magnetic storm, we also computed average values for only truly quiet events: those for which $Kp \leq 1$ and for which SYM-H > -30 nT. These comprised 1185 intervals, and the probability is shown as the diamonds in Figure 13. There is not much difference between this and the distribution for all quiet events. Table 2 summarizes the scaling exponents calculated for these distributions. For comparison, in Table 2 we have also divided the events into subsets that recognize the magnetic storm classification system of Table 1, and we have indicated the scaling exponents for

these cases. For the quiet events, for which the distribution is bi-Gaussian, we used the symbol α_1 to refer to the scaling exponent with the smaller value and α_2 for the exponent of larger value. It is evident from Table 2 that as the activity increases, there is an increase in the value of the mean scaling exponent.

4.3. Statistics for Independent Events

[31] As mentioned in section 4.2, it is not clear how the overlapping intervals will skew the results of the previous analysis, since the scaling exponents vary as a function of time and reflect nonlinear behavior under changing conditions. Some degree of bias will certainly result. In order to validate the use of overlapping intervals, in this section it is also necessary to consider the statistics when nonoverlapping (i.e., completely independent) intervals are used. There are a total of 76 active and 30 quiet intervals when data are completely independent. Figure 14 shows plots of the scaling exponents as a function of mean (top) and minimum (bottom) SYM-H. As before, data for active intervals are shown as pluses, and circles indicate data for quiet intervals.

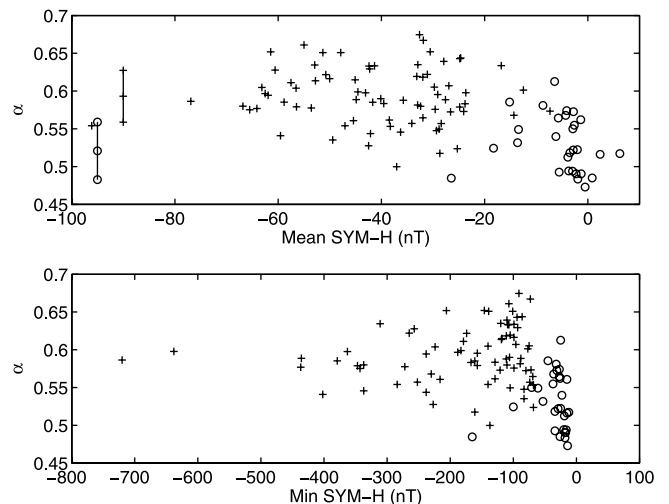


Figure 14. Comparison of computed α for quiet (circles) and active (pluses), as a function of mean and minimum SYM-H value for the data interval. Results shown here are from independent intervals. Quiet and active interval results cluster around different mean values, $\alpha_Q = 0.52 \pm 0.04$ and $\alpha_A = 0.59 \pm 0.03$, respectively. Average values are shown by the vertical lines to the left side of the plot.

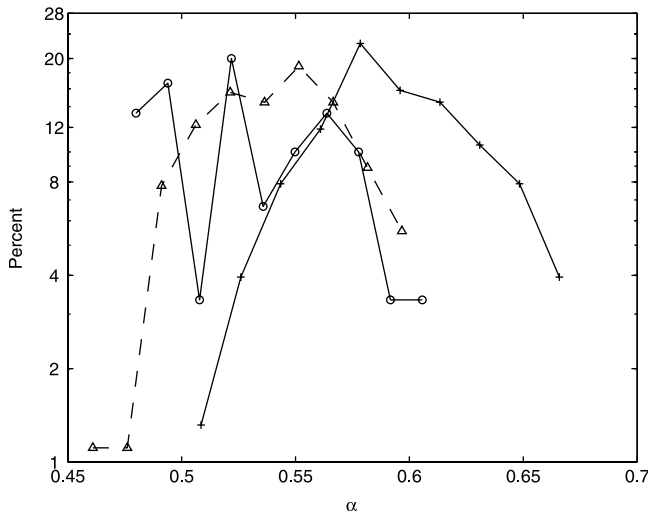


Figure 15. Probability distributions of the scaling exponents for active (pluses) and quiet (circles) events on a log scale. Results are from data intervals that were independent. Results from quiet events that had $Kp \leq 1.2$ are shown as triangles.

We find that there is no essential difference in our conclusions from overlapping data, although the average values change slightly: $\alpha_Q = 0.52 \pm 0.04$ and $\alpha_A = 0.59 \pm 0.03$. If anything, the differences in the means are more pronounced than before. Means and standard deviation error bars are shown at the left of Figure 14 (top). As before, we applied a Student's t test and found $p < 10^{-5}$.

[32] Because there are fewer events, the distribution for quiet intervals is not well resolved, as is shown in Figure 15. All distribution functions are normalized for comparison. The quiet data are shown as circles, and active data are shown as pluses. The active data have a well-resolved Gaussian distribution as before, which suggests that the bias for active intervals is not a large problem. This is because the distribution of the scaling exponent for overlapping intervals is similar for independent intervals.

[33] For quiet intervals (circles), there is some evidence for more than one peak, but the resolution is not good since there are too few data points. In order to better resolve the distribution for quiet intervals we relaxed the selection criterion and considered $Kp \leq 1.2$. For this case, 90 totally independent events are found, with an average scaling exponent $\alpha_Q = 0.54 \pm 0.03$. The normalized distribution is shown as the curve with triangles in Figure 15 and recovers the bi-Gaussian distribution as for the analysis with overlapping intervals. The increase in the scaling exponent with increasing activity is again apparent, as for the analysis of data with overlapping intervals; for $Kp \leq 1.5$, there are 230 independent events and $\alpha_Q = 0.55 \pm 0.03$.

5. Summary and Conclusions

[34] In this paper we used detrended fluctuation analysis to determine long-range dependence in SYM-H data. This technique has the advantage that it is better able to deal with nonstationarities than typical methods, such as variance analysis. The idea of the method is to subtract possible

deterministic trends from the original time series and then analyze the fluctuation of the detrended data. In all cases we found that the detrended fluctuation functions were linear over ~ 2 decades in log-log space, and no crossover in scaling behavior was observed. Locally, SYM-H appears monofractal. This means that a single scaling controls the dynamics over a wide range of scales. However, there is clear evidence from our analysis that the scaling exponent varies as a function of time and changes as a result of magnetospheric dynamics. We found that there is significant difference between the scaling exponents calculated for quiet and active intervals.

[35] For quiet intervals, we required $Kp \leq 1$ for 10,000 consecutive minutes. Similarly, to qualify as an active interval required $Kp \geq 4$ for 10,000 consecutive minutes. Since “local” changes in scaling exponents can be observed through DFA, it may be important to consider all intervals (including those that include overlapping data from other intervals) to get a full view of the nonlinear characterization of SYM-H. For many cases the Kp criterion was satisfied for more than 10,000 consecutive minutes. When this happened, intervals were allowed to have overlapping data, resulting in a large number of events. The SYM-H data set includes over 11 million points from which we identified 5823 active intervals and 1580 quiet intervals. For overlapping data, the overall average for quiet intervals was $\alpha_Q = 0.53 \pm 0.04$. For the active intervals we found $\alpha_A = 0.59 \pm 0.04$. In order to validate the results from overlapping intervals we also considered the statistics for nonoverlapping intervals only. When no overlapping data were allowed (completely independent intervals), we found only 76 independent active intervals and 30 independent quiet intervals for the Kp selection criteria. For this case we found that there was no essential difference from our conclusions for averages from the overlapping intervals; for independent intervals, $\alpha_Q = 0.52 \pm 0.04$, and $\alpha_A = 0.59 \pm 0.03$.

[36] Irregular geomagnetic fluctuations, which may be reflected in the SYM-H index, can be generated in remote regions of the magnetosphere. They can be the direct result of changes in solar wind forcing, or they can be induced in combination with internal magnetosphere-ionosphere instabilities. We found that the quiet interval scaling exponents had a bi-Gaussian distribution and are thus more complex to understand than dynamics of the active intervals. These two distinct components found during quiet times may be indicative of different internal (magnetospheric) and external (solar wind) nonlinear forcings. For example, *Burlaga and Klein* [1986] reported that under some conditions the solar wind has $\alpha \sim 0.5$, consistent with homogeneous, isotropic, stationary turbulence. In the fits to the quiet interval bi-Gaussian distribution for overlapping intervals, the lower value exponent was found to have $\alpha_1 = 0.48 \pm 0.01$, which is consistent with this picture. On the other hand, the higher-value quiet exponent has $\alpha_2 = 0.54 \pm 0.03$, which is perhaps more representative of a process that is internal to the magnetosphere, although it is not clear what this process might be.

[37] *Ohtani et al.* [1995] reported $\alpha \sim 0.7$ for magnetic fluctuations associated with tail current disruption. *Consolini and Lui* [2000] also examined scaling properties of magnetic fluctuations in the magnetotail. They found a

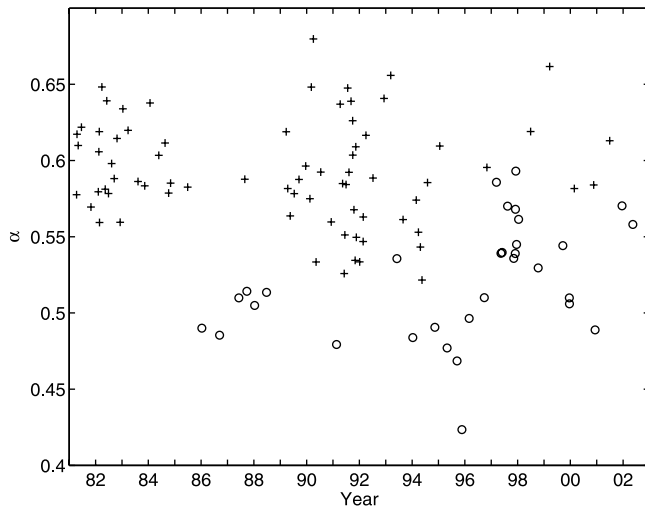


Figure 16. Averaged scaling exponents for quiet (circles) and active (pluses) events as a function of time from 1981 to 2002. Averaging is performed over active and quiet events that have overlapping intervals. That is, each circle and plus represents the average of numerous scaling exponents calculated for each one of these independent events.

scaling exponent $\alpha = 0.48 \pm 0.02$ before current disruption, changing to $\alpha = 0.70 \pm 0.02$ afterward. They concluded that the postdisruption statistics implied a persistent signal that may be the result of reorganization during current disruption. These results are similar to the results we have found for SYM-H statistics. The SYM-H scaling exponents calculated during quiet times are consistent with the pre-disruption scenario reported by *Consolini and Lui* [2000]. However, we found the new result that the quiet interval distribution has a bi-Gaussian nature. In this case the lower value, α_1 , quoted in the previous paragraph, is remarkably similar to the results for preonset reported by *Consolini and Lui* [2000]. As mentioned in section 4.2, the overall average for quiet intervals, assuming only a single Gaussian, was $\alpha = 0.53 \pm 0.04$, which is in accord with their results. The only difference here is the observation of the dual bi-Gaussian nature of the statistics. For the active intervals we found $\alpha = 0.59 \pm 0.04$. Although this is not the same as found for current disruption events by the above researchers, there is some similarity in that active events generally have larger nonlinear statistics than the quiet events. Indeed, as magnetospheric activity decreases, as measured in terms of SYM-H and Kp , so do the measured scaling exponents. The only exception is the 15 quiet events that have SYM-H < -100 nT, but these may be disregarded as statistically insignificant to make an impression on the larger general pattern that has been observed.

[38] Very similar distribution functions were found for the results for overlapping and independent intervals. The peaks for quiet and active intervals are clearly separated, and there is some overlap in the tails of the distributions. In order to determine whether the difference in the means from quiet and active intervals was significant, we applied a Student's t test. For results from both overlapping and independent intervals, we found $p < 10^{-5}$, which implies that the difference between the statistics computed for quiet and active intervals is statistically significant. The results show

that the averages for overlapping intervals and completely independent intervals are very similar. The distribution of nonlinear statistics for overlapping intervals is essentially the same as for independent intervals. This suggests that the scaling of SYM-H is the same over different locations in the time series, even when overlapping intervals are included.

[39] In Figure 16 we have averaged scaling exponents over the 22-year interval in this study. In Figure 16 the averaging was performed over active and quiet events that have overlapping intervals, although results for independent intervals are essentially the same. Each circle and plus represents the average of numerous scaling exponents calculated for each one of these independent events. In general, the quiet events feature smaller scaling exponents than for active events of similar epoch. This is important, because it lends support to the idea that quiet and active intervals are different in their nonlinear statistics. This graph also demonstrates strikingly that there is a temporal variation, although without any evidence of a dependence upon solar cycle. The most recent solar maxima were around approximately 2000 and 1990, and the most recent minima were around 1996 and 1986. For example, the scaling exponents for quiet events (circles) rises rather sharply around 1998. The ultimate significance or cause of this temporal variability is not clear and is not the concern of this study. It is, however, important to note that a temporal change of scaling exponent implies a symmetry breaking in a system in a state of self-organized criticality (SOC). This can occur when a system is perturbed near a critical point [Chang, 1992]. Our results do not demonstrate SOC by any means, but they are consistent with SOC. The difference in scaling exponents from quiet and active intervals suggests that the magnetosphere exists in a critical configuration. Transition to a lower energy state, such as a storm, thus results in more organization (larger scaling exponent) as the excess of energy is dissipated.

[40] All the active intervals we studied can be classified as magnetic storms. Magnetic storms could be understood as pathological features of the magnetosphere-ionosphere system, compared to the less active quiescent states. This study has thus quantified how the dynamical patterns of SYM-H fluctuations and associated scaling features change with such perturbations. Our findings raise the possibility that understanding SYM-H time-varying statistical alterations with magnetospheric activity has potential for magnetic storm prediction. For quiet intervals we found that the scaling exponents were not statistically different from 0.5. On the other hand, for active intervals, when the magnetosphere is strongly driven by the solar wind fluctuations, the average scaling exponent was significantly larger than 0.5. Since quiet time data are more representative of internal dynamics than active times, and since they have $\alpha \sim 0.5$, it suggests that whatever internal organization the system exhibits during quiet times is relatively weak.

[41] For active intervals we found that the scaling exponent is larger than 0.5, indicating greater correlation. As well, we noted in Table 1 that there appears to be a trend toward greater correlation, i.e., larger exponents, with increased activity. This may be representative of the organizing power of storms.

[42] We have found a significant difference between the scaling exponents for quiet and active intervals. This result

suggests that the SYM-H time series is inhomogeneous, resulting in different parts of the signal having different scaling properties. We have presented clear evidence that the roughness of the sample path for SYM-H varies with location. This means that a single number, α , may not provide an adequate global description of the roughness of the sample path. The fact that we have found significant differences in α , between quiet and active intervals, in the same data set, suggests that the basic dynamics of SYM-H could be captured by a modification to fBm. Peltier and Lévy-Véhel [1995] proposed such a scheme which they called MFBm. A feature of MFBm is that the sample path roughness is described by a function $\alpha(t)$ rather than a single number. Multifractional Brownian motion is a generalization of fractional Brownian motion in which the scaling exponent varies with time in the prescribed manner. The difference between quiet and active intervals indicates that the SYM-H time series, rather than being monofractal, is probably weakly multifractional. This result may be used as a predictive tool, since it may be that storm onsets are presaged by characteristic changes in the nonlinear scaling exponents, from values characteristic of quiet intervals to those characteristic of active intervals.

[43] **Acknowledgments.** SYM-H data are provided by the World Data Center for Geomagnetism, Kyoto. The research was funded under NSF grants ATM-0449403 and DMS-0417690. The author is grateful to the reviewers for excellent criticism that resulted in much deeper analysis of the data set.

[44] Lou-Chuang Lee thanks Channon Price and another reviewer for their assistance in evaluating this paper.

References

- Abramenko, V. I., V. B. Yurchyshyn, H. Wang, T. J. Spirock, and P. R. Goode (2002), Scaling behaviour of structure functions of the longitudinal magnetic field in active regions on the Sun, *Astrophys. J.*, *577*, 487.
- Baker, D. N., et al. (1997), Recurrent geomagnetic storms and relativistic electron enhancements in the outer magnetosphere: ISTP coordinated measurements, *J. Geophys. Res.*, *102*, 14,141.
- Bartels, J. (1963), Discussion of time variations of geomagnetic activity indices *Kp* and *Ap*, 1932–1961, *Ann. Geophys.*, *19*, 1.
- Benkevitch, L. V., W. B. Lyatsky, A. V. Koustov, G. J. Sofko, and A. M. Hamza (2002), Substorm onset times as derived from geomagnetic indices, *Geophys. Res. Lett.*, *29*(10), 1496, doi:10.1029/2001GL014386.
- Blok, H. J. (2000), *On the nature of the stock market: Simulations and experiments*, Ph.D. thesis, Univ. of B. C., Vancouver, B. C., Canada.
- Burlaga, L. F. (1991), Multifractal structure of the interplanetary magnetic field: Voyager 2 observations near 25 AU, 1987–1988, *Geophys. Res. Lett.*, *18*, 69.
- Burlaga, L. F., and L. W. Klein (1986), Fractal structure of the interplanetary magnetic field, *J. Geophys. Res.*, *91*, 347.
- Cannon, M. J., D. B. Percival, D. C. Caccia, G. M. Raymond, and J. B. Bassingthwaite (1997), Evaluating the scaled windowed variance methods for estimating the Hurst coefficient of time series, *Physica A*, *241*, 606.
- Chang, T. (1992), Low dimensional behavior and symmetry breaking of stochastic systems near criticality—Can these effects be observed in space and in the laboratory?, *IEEE Trans. Plasma Sci.*, *20*, 691.
- Chapman, S. (1919), An outline of the theory of magnetic storms, *Proc. R. Soc. London, Ser. A*, *95*, 61.
- Chen, Z., P. C. Ivanov, K. Hu, and H. E. Stanley (2002), Effect of non-stationarities on detrended fluctuation analysis, *Phys. Rev. E*, *65*, doi:10.1103/PhysRevE.65.041107.
- Collins, J. J., and C. J. De Luca (1994), Upright, correlated random walks: A statistical-biomechanics approach to human postural control system, *Chaos*, *5*(1), 57.
- Consolini, G., and A. T. Y. Lui (2000), Symmetry breaking and nonlinear wave-wave interaction in current disruption: Possible evidence for a phase transition, in *Magnetospheric Current Systems*, *Geophys. Monogr. Ser.*, vol. 118, edited by S.-I. Ohtani et al., p. 395, AGU, Washington, D. C.
- Daglis, I. A., R. M. Thorne, W. Baumjohann, and S. Orsini (1999), The terrestrial ring current: Origin, formation, and decay, *Rev. Geophys.*, *37*, 407.
- Daglis, I. A., J. U. Kozyra, Y. Kamide, D. Vassiliadis, A. S. Sharma, M. W. Liemohn, W. D. Gonzalez, B. T. Tsurutani, and G. Lu (2003), Intense space storms: Critical issues and open disputes, *J. Geophys. Res.*, *108*(A5), 1208, doi:10.1029/2002JA009722.
- Frisch, U. (1997), *Turbulence*, Cambridge Univ. Press, New York.
- Gonzalez, W. D., J. A. Joselyn, Y. Kamide, H. W. Kroehl, G. Rostoker, B. T. Tsurutani, and V. N. Vasyliunas (1994), What is a geomagnetic storm?, *J. Geophys. Res.*, *99*, 5771.
- Gosling, J. T., D. J. McComas, J. L. Phillips, and S. J. Bame (1991), Geomagnetic activity associated with Earth passage of interplanetary shock disturbances and coronal mass ejections, *J. Geophys. Res.*, *96*, 7831.
- Horne, R. B., and R. M. Thorne (2003), Relativistic electron acceleration and precipitation during resonant interactions with whistler-mode chorus, *Geophys. Res. Lett.*, *30*(10), 1527, doi:10.1029/2003GL016973.
- Hu, K., P. C. Ivanov, Z. Chen, P. Carpena, and H. E. Stanley (2001), Effect of trends on detrended fluctuation analysis, *Phys. Rev. E*, *64*, doi:10.1103/PhysRevE.64.011114.
- Hurst, H. E. (1951), The long term storage capacity of reservoirs, *Trans. Am. Soc. Civil. Eng.*, *116*, 770.
- Kamide, Y., et al. (1998), Current understanding of magnetic storms: Storm-substorm relationships, *J. Geophys. Res.*, *103*, 17,705.
- Kantelhardt, J. W., S. A. Zschiegner, E. Koscielny-Bunde, S. Havlin, A. Bunde, and H. E. Stanley (2002), Multifractal detrended fluctuation analysis of nonstationary time series, *Physica A*, *316*, 87.
- Kozyra, J. U., M. W. Liemohn, C. R. Clauer, A. J. Ridley, M. F. Thomsen, J. E. Borovsky, J. L. Roeder, V. K. Jordanova, and W. D. Gonzalez (2002), Multistep development and ring current composition changes during the 4–6 June 1991 magnetic storm, *J. Geophys. Res.*, *107*(A8), 1224, doi:10.1029/2001JA000023.
- Li, X., D. N. Baker, M. A. Temerin, T. E. Cayton, G. D. Reeves, R. A. Christensen, J. B. Blake, M. D. Looper, R. Nakamura, and S. G. Kanekal (1997), Multisatellite observations of the outer zone electron variation during the November 3–4, 1993, magnetic storm, *J. Geophys. Res.*, *102*, 14,123.
- Li, X., D. N. Baker, S. G. Kanekal, M. Looper, and M. Temerin (2001), SAMPEX long term observations of MeV electrons, *Geophys. Res. Lett.*, *28*, 3827.
- Liemohn, M. W., J. U. Kozyra, M. F. Thomsen, J. L. Roeder, G. Lu, J. E. Borovsky, and T. E. Cayton (2001), Dominant role of the asymmetric ring current in producing the storm time *Dst**, *J. Geophys. Res.*, *106*, 10,883.
- Lui, A. T. Y. (2002), Multiscale phenomena in the near-Earth magnetosphere, *J. Atmos. Sol. Terr. Phys.*, *64*, 125.
- Mandelbrot, B. B., and J. W. Van Ness (1968), Fractional Brownian motions, fractional noises and applications, *SIAM Rev.*, *10*, 422.
- Meredith, N. P., R. M. Thorne, R. B. Horne, D. Summers, B. J. Fraser, and R. R. Anderson (2003), Statistical analysis of relativistic electron energies for cyclotron resonance with EMIC waves observed on CRRES, *J. Geophys. Res.*, *108*(A6), 1250, doi:10.1029/2002JA009700.
- Muniandy, S. V., S. C. Lim, and R. Murugan (2001), Inhomogeneous scaling behaviors in Malaysian foreign currency exchange rates, *Physica A*, *301*, 407.
- Neuman, S. P., and V. Di Federico (2003), Multifaceted nature of hydrogeologic scaling and its interpretation, *Rev. Geophys.*, *41*(3), 1014, doi:10.1029/2003RG000130.
- Ohtani, S., T. Higuchi, A. T. Y. Lui, and K. Takahashi (1995), Magnetic fluctuations associated with tail current disruption: Fractal analysis, *J. Geophys. Res.*, *100*, 19,135.
- Peltier, R. F., and J. Lévy-Véhel (1995), Multifractional Brownian motion: Definition and preliminary results, *RR-2645*, Inst. Natl. de Rech. en Informatique et en Autom., Le Chesnay, France.
- Peng, C.-K., S. Havlin, H. E. Stanley, and A. L. Goldberger (1995), Quantification of scaling exponents and crossover phenomena in nonstationary heartbeat timeseries, *Chaos*, *5*(1), 82.
- Price, C. P., and D. E. Newman (2001), Using the R/S statistic to analyze AE data, *J. Atmos. Sol. Terr. Phys.*, *63*, 1387.
- Rangarajan, G. K., and T. Iyemori (1997), Time variations of geomagnetic activity indices *Kp* and *Ap*: An update, *Ann. Geophys.*, *15*, 1271.
- Reeves, G. D. (1998), Relativistic electrons and magnetic storms: 1992–1995, *Geophys. Res. Lett.*, *25*, 1817.
- Reeves, G. D., and M. G. Henderson (2001), The storm-substorm relationship: Ion injections in geosynchronous measurements and composite energetic neutral atom images, *J. Geophys. Res.*, *106*, 5833.
- Richardson, I. G., E. W. Cliver, and H. V. Cane (2001), Sources of geomagnetic storms for solar minimum and maximum conditions during 1972–2000, *Geophys. Res. Lett.*, *28*, 2569.
- Sharma, A. S. (1995), Assessing the magnetosphere's nonlinear behavior: Its dimension is low, its predictability, high, *Rev. Geophys.*, *33*, 645.
- Summers, D., C. Ma, N. P. Meredith, R. B. Horne, R. M. Thorne, D. Heynderickx, and R. R. Anderson (2002), Model of the energization of outer-zone electrons by whistler-mode chorus during the

- October 9, 1990 geomagnetic storm, *Geophys. Res. Lett.*, 29(24), 2174, doi:10.1029/2002GL016039.
- Taqqu, M. S., V. Teverovsky, and W. Willinger (1996), Estimators for long-range dependence: An empirical study, *Fractals*, 3, 185.
- Taqqu, M., V. Teverovsky, and W. Willinger (1997), Is network traffic self-similar or multifractal?, *Fractals*, 5, 63.
- Tsurutani, B. T., W. D. Gonzalez, F. Tang, and Y. T. Lee (1992), Great magnetic storms, *Geophys. Res. Lett.*, 19, 73.
- Vandewalle, N., and M. Ausloos (1997), Coherent and random sequences in financial fluctuations, *Physica A*, 246, 454.
- Vjushin, D., R. B. Govindan, R. A. Monetti, S. Havlin, and A. Bunde (2001), Scaling analysis of trends using DFA, *Physica A*, 302, 234.
- Wanliss, J. A. (2004), Nonlinear statistical precursors to magnetic storm onset, paper presented at Conference on Sun-Earth Connections, Johns Hopkins Univ. Appl. Phys. Lab., Kona, Hawaii.
- Wanliss, J. A., and M. A. Reynolds (2003), Measurement of the stochasticity of low-latitude geomagnetic temporal variations, *Ann. Geophys.*, 21, 2025.

J. Wanliss, Department of Physical Sciences, Embry-Riddle Aeronautical University, 600 S. Clyde Morris Blvd., Daytona Beach, FL 32114, USA. (james.wanliss@erau.edu)